A Sample Time Optimization Problem in a Digital Control System

Wojciech Mitkowski and Krzysztof Oprzędkiewicz

Abstract In the paper a phenomenon of the existence of a sample time minimizing the settling time in a digital control system is described. As a control plant an experimental heat object was used. The control system was built with the use of a soft PLC system SIEMENS SIMATIC. As the control algorithm a finite dimensional dynamic compensator was applied. During tests of the control system it was observed that there exists a value of the sample time which minimizes the settling time in the system. This phenomenon is tried to explain.

1 Introduction

In the paper a digital control system for an experimental heat control plant is considered. The control plant is shown in Fig. 1. It has the form of a thin copper rod 30 cm long with an electric heater of length Δx_u localized at one end and resistive temperature sensor of length Δx at the other end. The input signal of the system is the standard current signal 0 – 5 [mA]. It is amplified to the range 0 – 1.5 [A] and it is the input signal for the heater. The temperature of the rod is measured with the use of a resistance sensor. The signal from the sensor is transformed to the standard current signal 0 – 5 [mA] with the use of a transducer.

The structure of the digital control system is shown in Fig. 2. In this figure $y^+(k) = y(kh), h > 0, k = 0,1,2,\ldots$ and $u(t) = u^+(k)$ for $t \in [kh,\ (k+1)h)$, $h > 0$ denotes the sample time of D/A and A/D converters working synchronically. During tests of this control system it was observed that the settling time (after this time the difference between the seat point r and the process value $y(t)$ is stably smaller than 5%) is a function of the sample time $h > 0$, $t_k = kh$, $k = 0,1,2,\ldots$, and this function

Wojciech Mitkowski
Institute of Automatics, AGH University of Science and Technology, e-mail: wmi@ia.agh.edu.pl

Krzysztof Oprzędkiewicz
Institute of Automatics, AGH University of Science and Technology, e-mail: kop@agh.edu.pl

has a minimum. This means that there exists a value of the sample time minimizing the settling time, which is one of fundamental direct control cost functions, applied in the industrial practice.

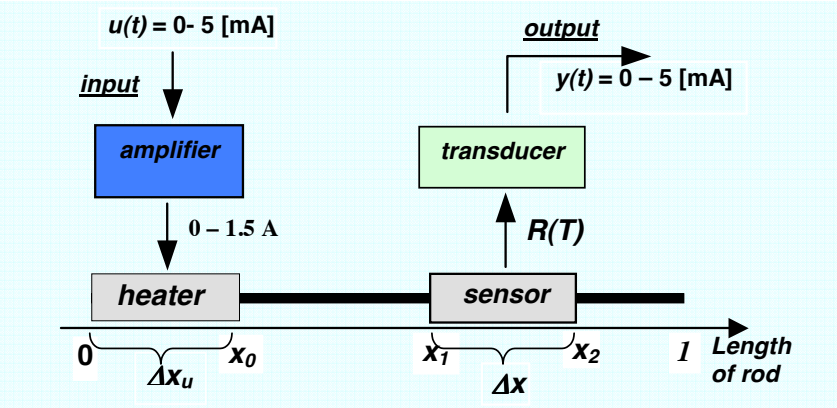

Fig. 1 The experimental heat control plant

This effect was observed during tests of a discrete, finite-dimensional dynamic compensator. The control algorithm is based on the mathematical model of the control plant shown in Fig. 1, the control algorithm was implemented at the SIEMENS multipanel based "soft PLC" system. The hardware and software scheme of this system is shown in Fig. 6. In the control system shown in Fig. 2, D/A and A/D converters work synchronically.

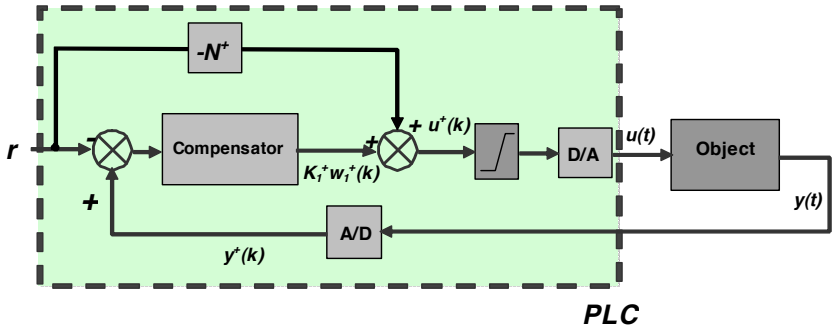

Fig. 2 The structure of the control system.

In this paper the existence of the sample time minimizing the settling time is tried to explain. A method of optimal sample time determination for the considered control system is also proposed.

2 The Mathematical Model of the Control Plant

The mathematical model of the control plant we deal with is the following heat transfer equation:

$$\begin{aligned}
&\tfrac{\partial T(x,t)}{\partial t} = a\tfrac{\partial^2 T(x,t)}{\partial x^2} - R_a T(x,t) + b(x)u(t), \quad 0 \le x \le 1, \quad t \ge 0\\
&\tfrac{\partial T(0,t)}{\partial x} = 0, \quad \tfrac{\partial T(1,t)}{\partial x} = 0, \quad t \ge 0\\
&T(x,0) = 0, \quad 0 \le x \le 1\\
&y(t) = y_0 \int_0^1 T(x,t)c(x)\,dx
\end{aligned} \tag{1}$$

where $T(x,t)$ denotes the temperature of the rod at the point $x \in [0,1]$ and time moment t, a and R_a are the suitable heat transfer coefficients. All variables and constants are dimensionless. The coefficient R_a describes the heat exchange along the side surface of the rod. The coefficient y_0 is the gain of the slotted line. The heat exchange at the ends of rod is much smaller than along the side surface and it can be described by the homogeneous Neumann's boundary conditions. To make the model simpler, the length of the rod was assumed equal to one: $x \in [0,1]$. The diameter of the rod is much smaller than its length, that is why in equation (1) only length of rod x is considered. The control and observation in the plant we deal with (see Fig. 1) are distributed. Both the heater characteristic function $b(x)$ and sensor characteristic function $c(x)$ depend on the length of these elements. The length of the heater is equal to $\Delta x_u = 1/13$ and its characteristic function is as follows:

$$b(x) = \begin{cases} 1 & \text{for } x \in (0,x_0) \\ 0 & \text{for } x \notin (0,x_0) \end{cases} \tag{2}$$

where $x_0 = 1/13$. The temperature of the rod is measured in the segment $\Delta x = x_2 - x_1 = 1/13$ (distributed observation). The temperature sensor is described by the following characteristic function:

$$c(x) = \begin{cases} 1 & \text{for } x \in (x_1,x_2) \\ 0 & \text{for } x \notin (x_1,x_2) \end{cases} \tag{3}$$

where $x_1 = 25/52$, $x_2 = 27/52$.

The above model was tested in laboratory (see Fig. 3) and discussed in a number of previous papers, for example in [9, 10, 8]. The practical realization of control and observation justifies the assumption that the control and observation are distributed. This also simplifies the mathematical model of the plant. An interesting example of analysis of this problem with pointwise control and observation was presented by Grabowski in 1997 [1].

The numerical values of the heat exchange coefficients a and R_a were calculated with the use of the least squares method and the experimental step response of the plant (see [9]). They are equal to a= 0.000945, R_a= 0.0271. The idea of identification of the coefficients was to minimize (w.r.t. the parameters a and R_a) the following

cost function:

$$J_0(a,R_a)=\sum_{k=1}^{S}[y(kh)-\tilde{y}(kh)]^2 \tag{4}$$

where $kh,k=1,2,3,\ldots,S$ are discrete time moments, $y(kh)$ is the output of (1) for the control signal $u(t)=1(t)$, $\tilde{y}(kh)$ is the step response of the real plant (see Fig. 1) measured at discrete time moments $kh,k=1,2,3,\ldots,S$. During the identification experiment the sample time h was equal to 0.1 [s] and the number of samples S was equal to 3000.

The value of the steady-state gain y_0 was calculated via comparison of $y(kh)$ with $\tilde{y}(kh)$ after a suitably long time $t_S=Sh$. The value of this gain is equal to 25.7922.

Let $L(U,X)$ denote the space of linear continuous operators $S:U\rightarrow X$ with the following natural norm: $||S||=\sup\{||Sv||_X:\ ||v||_U\leq 1\}$. Let $X=L^2(0,1;\mathbb{R})$ be a Hilbert space with scalar product $(p\mid d)=\int_0^1 p(x)d(x)dx$. The boundary problem (1) can be interpreted ([12], [11], p. 106; [2], p. 488) as the following differential equation in the Hilbert space $L^2(0,1;\mathbb{R})$:

$$\begin{aligned}&\dot{T}(t)=AT(t)+Bu(t),\quad T(0)=0,\quad 0\leq t\\&y(t)=CT(t)\end{aligned} \tag{5}$$

where $T(t)\in X=L^2(0,1;\mathbb{R})$, $u(t)\in\mathbb{R}=U$, $y(t)\in\mathbb{R}=Y$, $B\in L(U,X)$, $(Bu(t))(x)=b(x)u(t)$, $C\in L(X,Y)$, $CT(t)=y_0\ (T(t)|c)$, A is a linear operator with the domain $D(A)$:

$$\begin{aligned}&Aw=aw''-R_aw,\quad w''(x)=d^2w(x)/dx^2,\\&D(A)=\{w\in X:\ w''\in X,w'(0)=0,w'(1)=0\}\end{aligned} \tag{6}$$

The operator defined by (6) is self-adjoint and has a compact resolvent. This implies that A is a discrete operator. The spectrum of a discrete operator consists only of isolated eigenvalues and all eigenvalues have finite multiplicities. The operator given by (6) has a discrete spectrum with the simple eigenvalues:

$$\lambda_i=-i^2a\pi^2-R_a,\quad i=0,1,2,3,\ldots \tag{7}$$

Eigenvectors associated with the eigenvalues (7) are defined as follows:

$$w_i(x)=\begin{cases}1, & i=0\\ \sqrt{2}\cos(i\pi x), & i=1,2,\ldots\end{cases} \tag{8}$$

The eigenvectors (8) build an orthonormal basis of the space $X=L^2(0,1;\mathbb{R})$.

If the basis of $X=L^2(0,1;\mathbb{R})$ is built by the set of eigenvectors (8), then the operators A,B and C in (5) can be expressed as the following infinite-dimensional matrices (see [13]):

$$A=diag\{\lambda_0,\lambda_1,\lambda_2,\ldots\},\quad B=[b_0\ b_1\ b_2\ldots]^T,\quad C=y_0[c_0\ c_1\ c_2\ldots] \tag{9}$$

where $b_i = \int_0^1 b(x)w_i(x)dx = (b|w_i)$, $c_i = \int_0^1 c(x)w_i(x)dx = (c|w_i)$, $i = 0,1,2,\ldots$.

The operator (6) is the generator of an analytical, exponentially stable C_0- semigroup e^{At}, $t \geq 0$ in the space $X = L^2(0,1;\mathbb{R})$, where:

$$e^{At}w = \sum_{i=0}^{\infty} e^{\lambda_i t}(w|w_i)w_i \tag{10}$$

The analysis of (7) and (10) justifies the use of finite-dimensional approximation of (5). Instead of $i = 0,\ 1,\ 2,\ 3,\ \ldots$ we will use: $i = 0,\ 1,\ 2,\ 3,\ \ldots\ , N$. A suitable value of N for finite-dimensional approximation is N= 25 (see [9]). The respective finite-dimensional matrix representations of the operators A, B and C for the presented model (5) are as follows:

A = diag $(-0.0271, -0.0364, -0.0644, -0.1110, -0.1763, -0.2603, -0.3629,$
$-0.4841, -0.6240, -0.7826, -0.9598, -1.1556, -1.3702, -1.6033, -1.8551,$
$-2.1256, -2.4148, -2.7225, -3.0490, -3.3941, -3.7578, -4.1402, -4.5413,$
$-4.9610, -5.3993)$,

$B = \text{col}\,(\ 0.0769,\ 0.1077,\ 0.1046,\ 0.0995,\ 0.0926,\ 0.0842,\ 0.0745,$
$0.0638,\ 0.0526,\ 0.0412,\ 0.0299,\ 0.0190,\ 0.0090,\ 0.0000, -0.0077,$
$-0.0139, -0.0187, -0.0218, -0.0234, -0.0235, -0.0223, -0.0200, -0.0168,$
$-0.0130, -0.0087)$,

$C^\top = \text{col}\,(\ 0.9920,\ 0.0000, -1.3995,\ 0.0000,\ 1.3893,\ 0.0000, -1.3724,$
$0.0000,\ 1.3489,\ 0.0000, -1.3191,\ 0.0000,\ 1.2832,\ 0.0000, -1.2415,$
$0.0000,\ 1.1944,\ 0.0000, -1.1423,\ 0.0000,\ 1.0856,\ 0.0000, -1.0248,$
$0.0000,\ 0.9605)$.

The form of operators (9) enables the decomposition of the system (5) into an infinite number of one-dimensional subsystems. Notice that the matrices B and C contain zero elements. This implies that the finite-dimensional approximation is both uncontrollable and unobservable, but the subsystems containing suitable nonzero elements of B and C are controllable and observable.

3 Digital Control System

The scheme of the digital control system is shown in Fig. 2. Both D/A and A/D converters work synchronically with the sample time $h > 0$ and their work can be described as follows: $y^+(k) = y(kh)$ and $u(t) = u^+(k)$ for$t \in [kh,\ (k+1)h)$, where $k = 0,1,2,\ldots$. The serial connection of a D/A converter, a continuous control plant and an A/D converter builds the discrete system described as follows (see, for example, [7], p. 140, 236):

$$T^+(k+1) = A^+T^+(k) + B^+u^+(k), \quad y^+(k) = C^+T^+(k) \tag{11}$$

where $k = 0,1,2,\ldots$

$$A^+ = e^{Ah}, \quad B^+ = \int_0^h e^{At} B\,dt, \quad C^+ = C \tag{12}$$

and the matrices A, B and C are described by (9).

For the discrete system (11), the finite-dimensional discrete compensator proposed in [3] (p. 60), [4, 5, 6], or [7] (p. 236) can be built (see Fig. 2). The nonlinear element (saturation) is necessary to describe the technical realization of control, because real control signals are always bounded. The control system with the dynamic compensator and bounded control signal was discussed by Mitkowski and Oprzędkiewicz in 1999 [8].

Notice that the matrices B^+ and $C^+ = C$ contain zero elements. This implies that the system is neither controllable nor observable. The damping coefficients can be improved only in controllable and observable subsystems.

Let $T^+(k) = T(kh)$, where $k = 0,1,2,\ldots$. Equations (9) and (12) allow us to make the following decomposition of the system (11):

$$\begin{bmatrix} T_1^+(k+1) \\ T_2^+(k+1) \\ T_3^+(k+1) \end{bmatrix} = \begin{bmatrix} A_1^+ & 0 & 0 \\ 0 & A_2^+ & 0 \\ 0 & 0 & A_3^+ \end{bmatrix} \begin{bmatrix} T_1^+(k) \\ T_2^+(k) \\ T_3^+(k) \end{bmatrix} + \begin{bmatrix} B_1^+ \\ B_2^+ \\ B_3^+ \end{bmatrix} u^+(k),$$
$$y^+(k) = C_1^+ T_1^+(k) + C_2^+ T_2^+(k) + C_3^+ T_3^+(k) \tag{13}$$

where $T_i^+(k) \in X_i$, $i = 1,2,3$, $\dim X_1 < +\infty, \dim X_2 = p < +\infty, \dim X_3 = +\infty$.

For further considerations a finite-dimensional approximation with $N = 25$ and example value of sample time $h = 5$ [s] will be applied. Using the equations (12) we obtain the following values of matrices for the system after discretization:

$A^+ = \mathrm{diag}\,(0.8733,\ 0.8335,\ 0.7247,\ 0.5740,\ 0.4141,\ 0.2722,\ 0.1629,\ 0.0889,$
$0.0442,\ 0.0200,\ 0.0082,\ 0.0031,\ 0.0011,\ 0.0003,\ 0.0001,\ 0.0000,\ 0.0000,$
$0.0000,\ 0.0000,\ 0.0000,\ 0.0000,\ 0.0000,\ 0.0000,\ 0.0000,\ 0.0000),$

$B^+ = \mathrm{col}\,(0.3597,\ 0.4924,\ 0.4471,\ 0.3818,\ 0.3077,\ 0.2354,\ 0.1718,\ 0.1201,$
$0.0806,\ 0.0515,\ 0.0308,\ 0.0164,\ 0.0065,\ 0.0000,-0.0041,-0.0066,-0.0077,$
$-0.0080,-0.0077,-0.0069,-0.0059,-0.0048,-0.0037,-0.0026,-0.0016).$

As both D/A and A/D converters work synchronically, then $C^+ = C$.

In the scheme of Fig. 2, r denotes the seat point in the system, $y(t)$ denotes the system's output (the process value), $u(t)$ denotes the control signal, $y^+(k)$ and $u^+(k)$ denote discrete versions of control and output. The difference $y^+(k) - r$ describes the error in the control system. The compensator is described as follows:

$$\begin{bmatrix} w_1^+(k+1) \\ w_2^+(k+2) \end{bmatrix} = A_S^+ \cdot \begin{bmatrix} w_1^+(k) \\ w_2^+(k) \end{bmatrix} + B_S^+ \left[y^+(k) - r \right]$$
$$u^+(k) = K_1^+ w_1^+(k) + N^+ r \tag{14}$$

where

$$A_S^+ = \begin{bmatrix} A_1^+ - G_1^+ C_1^+ + B_1^+ K_1^+ & -G_1^+ C_2^+ \\ B_2^+ K_1^+ & A_2^+ \end{bmatrix}, \qquad B_S^+ = \begin{bmatrix} G_1^+ \\ 0 \end{bmatrix} \tag{15}$$

In (14) and (15) $w_1^+(k)$, $w_2^+(k)$ denote the state variables of the compensator, the constant N^+ should assure the steady-state error equal to zero (after a suitably long time $y(t) = r$ for the seat point $r = const$). The dynamics of the whole closed-loop control system is described by transient states, the same for increasing and decreasing values of r.

The whole closed-loop system of Fig. 2 for $r = 0$ and without the nonlinear element can be described as underneath:

$$\begin{bmatrix} e_1^+(k+1) \\ e_2^+(k+1) \\ T_1^+(k+1) \\ T_2^+(k+1) \\ T_3^+(k+1) \end{bmatrix} = \begin{bmatrix} A_1^+ - G_1^+ C_1^+ & -G_1^+ C_2^+ & 0 & 0 & -G_1^+ C_3^+ \\ 0 & A_2^+ & 0 & 0 & 0 \\ B_1^+ K_1^+ & 0 & A_1^+ + B_1^+ K_1^+ & 0 & 0 \\ B_2^+ K_1^+ & 0 & B_2^+ K_1^+ & A_2^+ & 0 \\ B_3^+ K_1^+ & 0 & B_3^+ K_1^+ & 0 & A_3^+ \end{bmatrix} \begin{bmatrix} e_1^+(k) \\ e_2^+(k) \\ T_1^+(k) \\ T_2^+(k) \\ T_3^+(k) \end{bmatrix}$$

$$e_i^+(k) = w_i^+(k) - T_i^+(k), \quad i = 1, 2 \tag{16}$$

where $k = 0,\ 1,\ 2,\ \ldots$. Notice that the state operator:

$$A^+ = blocdiag(A_1^+, A_2^+, A_3^+) \tag{17}$$

of the system (13) is diagonal and it has a discrete spectrum containing the following eigenvalues:

$$\lambda_i^+ = e^{\lambda_i h}, \quad i = 0,\ 1,\ 2,\ \ldots, \tag{18}$$

where λ_i is expressed by (7), $h > 0$. This implies that $|\lambda_i^+| < 1$ and the discrete system (13) is asymptotically stable. The state operator of the discrete system (16) has the following form:

$$\tilde{A}^+ = blocdiag(A_1^+, A_2^+, A_1^+, A_2^+, A_3^+) + D \tag{19}$$

where D is a bounded operator (it describes a bounded perturbation of A^+). This implies that the operator $\tilde{A}^+$ has a discrete spectrum only.

The discrete system (16) with discrete operator $\tilde{A}^+$ is asymptotically stable, if its discrete spectrum is localized inside the unit circle: $|\lambda(\tilde{A}^+)| < 1$. The matrices A_1^+ and A_2^+ are finite-dimensional. The matrices G_1^+ and K_1^+ should assure the meeting of the following condition:

$$|\lambda(A_1^+ - G_1^+ C_1^+)| < 1 \quad \text{and} \quad |\lambda(A_1^+ + B_1^+ K_1^+)| < 1 \tag{20}$$

This condition can be fulfilled only if the suitable subsystems are controllable and observable.

In particular, the matrices G_1^+ and K_1^+ can be assigned to assure the eigenvalues of $A_1^+ - G_1^+ C_1^+$ and $A_1^+ + B_1^+ K_1^+$ equal to zero. Furthermore, when the dimension of A_1^+ is equal to 1 ($\dim X_1 = 1$ in equation (13)), the matrices G_1^+ and K_1^+, assuring eigenvalues equal to zero turn to real numbers equal to

$$G_1^+ = \frac{A_1^+}{C_1^+} = \frac{\lambda_0^+}{y_0 c_0}, \quad K_1^+ = -\frac{A_1^+}{B_1^+} = -\frac{\lambda_0^+}{b_0^+} \tag{21}$$

In (21), $\lambda_0^+ = e^{\lambda_0 h}$ denotes the first, most poorly damped element of the discrete system's spectrum, y_0, c_0 and b_0^+ denote suitable elements of output and control matrices for discrete system.

Denote the maximal eigenvalue of A_2^+ by $\lambda_{\max}^+ = \max \lambda (A_2^+)$. Notice that if $||C_3^+|| \to 0$ for $\dim X_2 \to +\infty$, then the bounded perturbation theorem implies the existence of such a $p < +\infty$ that the discrete system (16) is exponentially stable with a damping coefficient $\gamma \in (\lambda_{\max}^+, \lambda_0^+)$.

Generally, the construction of feedback (14), (15) consists in calculating the matrices K_1^+ and G_1^+. It can be done with the use of finite-dimensional approach, for example LQ (see [7], pp. 71, 78). The assumed damping coefficient can be obtained by increasing the dimension of the subsystem X_2: $p = \dim X_2$. The constant N^+ is calculated to assure the steady-state error in the control system equal to zero.

4 The Sample Time Optimization

Assume for further considerations that $\dim X_1 = 1$ and $p = \dim X_2 = 2$. The subsystem X_1 is controllable and observable, because $b_0 \neq 0$ and $y_0 c_0 \neq 0$ (see (12)). Then from (21) we obtain:

$$G_1^+ = \frac{e^{-R_a h}}{y_0 c_0}, \quad K_1^+ = \frac{R_a e^{-R_a h}}{b_0 \left(e^{-R_a h} - 1\right)} \tag{22}$$

The coefficients G_1^+ and K_1^+ of the compensator (14) are functions both of plant's parameters and sample time $h > 0$.

5 Experiments

The general hardware and software scheme of the laboratory control system is shown in Fig. 3, the scheme of the control plant is shown in Fig. 1.

The control system with the compensator for the plant shown in Fig. 1 was implemented on the "soft PLC" platform shown in Fig. 6. During experiments a servo problem was tested. Example experimental plots of the seat point r, the control signal $u(t)$ and the output $y(t)$ are shown in Fig. 4. They were obtained after a step

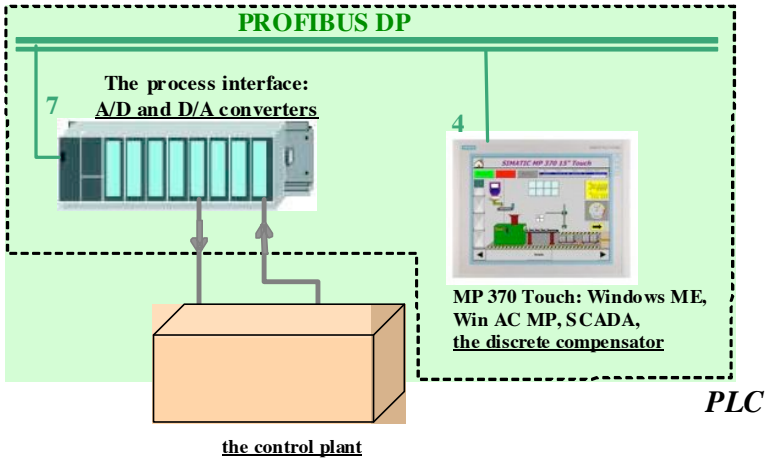

Fig. 3 The hardware and software scheme of the laboratory control system.

change of the seat point from the value $r = 0.25$ [mA] to $r = 1.75$ [mA]. The sample time h was equal to 723 [ms].

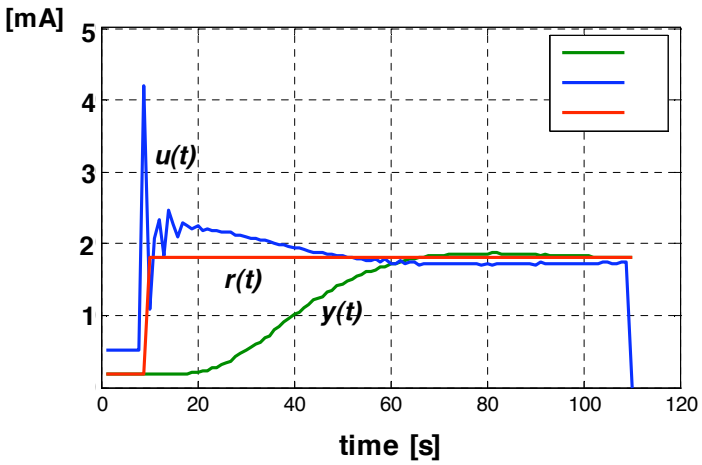

Fig. 4 Plots of $y(t)$, $u(t)$ and r in the considered control system.

The settling time is a time, after which the error in the control system (the difference between the seat point r and the system's output $y(t)$) is stably smaller than 5%. It will be denoted by T_c. Experimentally determined values of the settling time in the considered control system are presented in Table 2.

With the use of the above experimental results interpolation polynomials were built. The following polynomials were considered:

Table 1 Experimentally determined values of settling time T_c

Sample time h [ms]	settling time T_c[s]
300	52.37
400	50.52
500	49.17
600	48.35
700	48.01
800	48.17
900	48.73
1000	50.05

$$\begin{aligned} W_2(h) &= a_2 h^2 + a_1 h + a_0 \\ W_3(h) &= a_3 h^3 + a_2 h^2 + a_1 h + a_0 \\ W_5(h) &= a_5 h^5 + a_4 h^4 + a_3 h^3 + a_2 h^2 + a_1 h + a_0 \end{aligned} \tag{23}$$

Numerical values of coefficients of polynomials (23) are given in Table 2.

Table 2 Coefficients of interpolation polynomials (23)

W_2	W_3	W_5
		$a_5 = 9.0705 \cdot 10^{-14}$
	$a_3 = 1.8434 \cdot 10^{-9}$	$a_4 = -2.7670 \cdot 10^{-14}$
$a_2 = 2.5220 \cdot 10^{-5}$	$a_2 = 2.1626 \cdot 10^{-5}$	$a_3 = 3.2368 \cdot 10^{-7}$
$a_1 = -0.0362$	$a_1 = -0.0340$	$a_2 = -1.5593 \cdot 10^{-4}$
$a_0 = 60.9604$	$a_0 = 60.5650$	$a_1 = 0.0123$
		$a_0 = 55.9942$

The settling time T_c as a function of the sample time h, and all its interpolations are presented in Fig. 5.

Polynomials (23) were applied to estimate the values of sample time h minimizing the settling time T_c. The estimated optimal values of h are presented in Table 4. In the same table the experimentally determined values of settling time for the optimal estimated sample times are also presented.

Table 3 Values of sample time h and corresponding values of settling time T_c , determined experimentally and estimated with the use of polynomials (23)

Polynomial	W_2	W_3	W_5
Estimated optimal sample time [ms]	715	721	723
Estimated optimal settling time [s]	47.98	47.97	48.02
Experimentally determined settling time for estimated optimal sample time [s]	48.17	48.13	48.12

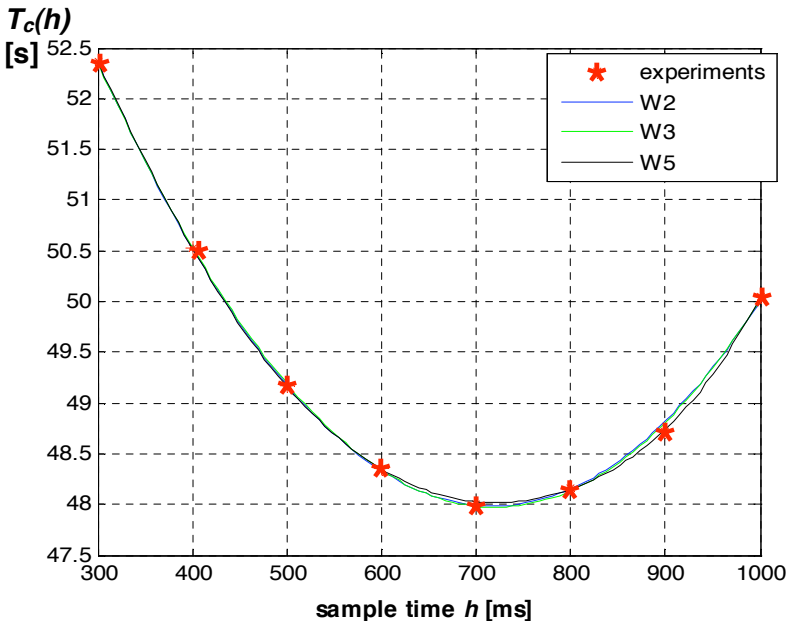

Fig. 5 The settling time T_c as a function of sample time h – experiments and all interpolation polynomials.

From the diagrams in Fig. 5 and Table 5 we can conclude that the estimated and experimental results are very close.

6 Simulations

The control system described in the previous section was also tested with the use of MATLAB/SIMULINK. During simulations the dependence of the settling time T_c on the sample time h was tested. The SIMULINK model of the control system is shown in Fig. 6. The simulation parameters were as follows: the stop time 300[s], numerical method: Ode 45 (Dormand Prince), variable step, minimal step size: 0.005[s], maximal step size: 0.01[s], initial step size: 0.01[s].

The settling time T_c as a function of the sample time h is shown in Table 6 and in Fig. 7.

The minimal value of the function shown in Fig. 7 is localized between $h = 12.6$ [s] and $h = 12.8$ [s].

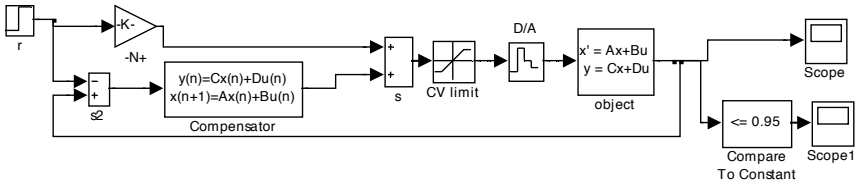

Fig. 6 The SIMULINK model of the control system.

Table 4 The settling time as a function of the sample time

sample time h [s]	settling time T_c [s]
12.0	69.92
12.1	69.83
12.2	69.75
12.3	69.69
12.4	69.64
12.5	69.61
12.6	69.59
12.7	69.59
12.8	69.59
12.9	69.6
13.0	69.63
13.1	69.66
13.2	69.70

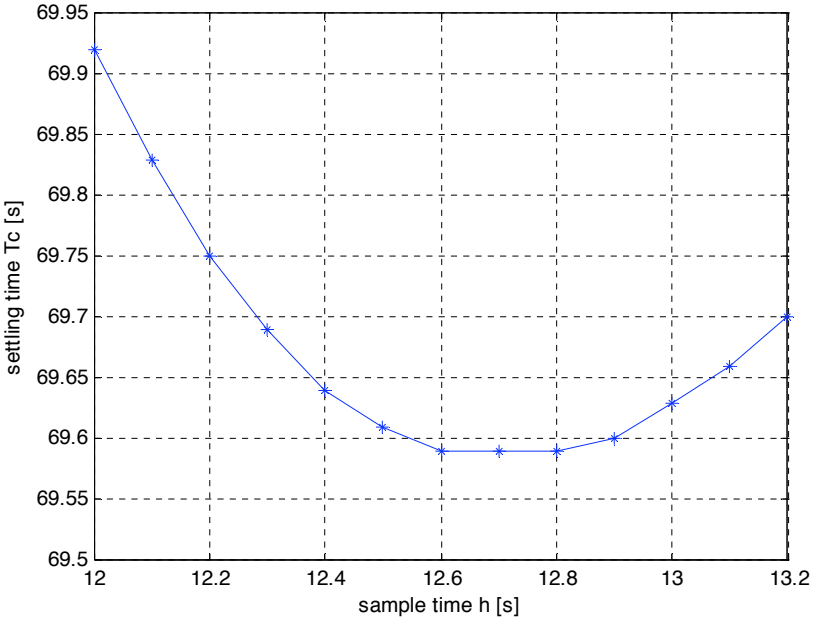

Fig. 7 The settling time T_c as a function of the sample time h.

7 A Comparison with a Weighted Cost Function

Consider the cost function $J(h)$ proposed in [3], p. 61, [4] and [7], p. 241:

$$J(h) = \left\| G_1^+(h) \right\| + \left\| K_1^+(h) \right\| + \alpha h \tag{24}$$

This cost function is a weighted sum of the settling time, approximately expressed by the term αh and the norms $||G_1^+||$ and $||K_1^+||$ describing gain coefficients of the discrete compensator (14). For the particular case, if G_1^+ and K_1^+ are described by (22), the cost function (24) has the following form:

$$J(h) = \frac{e^{-R_a h}}{y_0 c_0} + \frac{R_a e^{-R_a h}}{b_0 (1 - e^{-R_a h})} + \alpha h \tag{25}$$

where c_0 and b_0 are appropriate elements of the output and control matrices.

The cost function (25) depends on model's parameters and sample time $h > 0$. An example diagram of function (25) for the considered object parameters, weight coefficient $\alpha = 25$ and range of sample time h from 0.5 to 1.0 [s] is shown in Fig. 8.

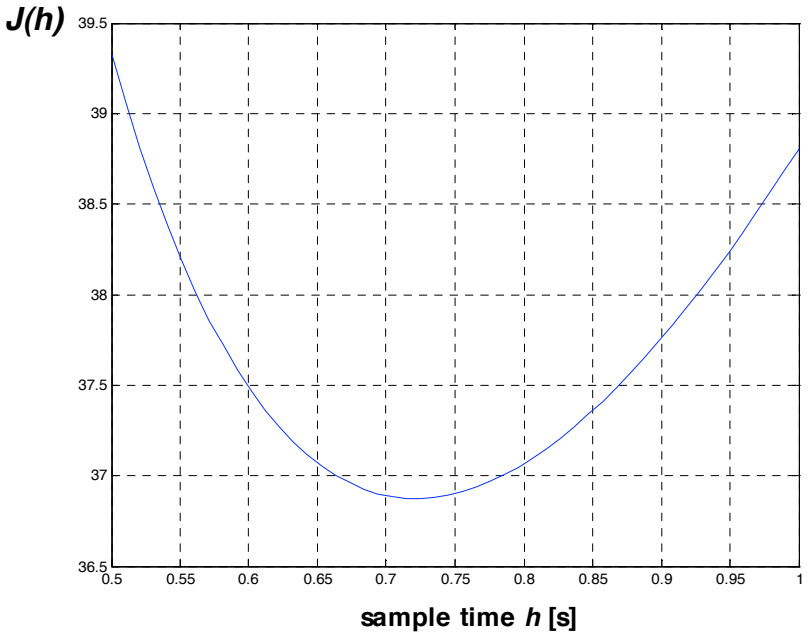

Fig. 8 The cost function (25) as a function of sample time h.

The value h_{opt} of the sample time h minimizing the function shown in Fig. 8 was calculated numerically and it is equal to

$$h_{opt} = 0.7216 \tag{26}$$

The value of function (25) for the sample time h_{opt} is equal to

$$J(h_{opt}) = 36.8738 \tag{27}$$

The comparison of the cost function (25) proposed theoretically and shown in Fig. 8 with the experimental results shown in Fig. 5 allows us to conclude that the value of the sample time h_{opt} minimizing the cost function (25) is equal to the value of h, which minimizes the interpolating polynomial W_3. The value of $J(h_{opt})$ is smaller than $T_c(h_{opt})$, because the function J does not express the settling time.

Furthermore, the general form of the dependence of the settling time T_c on the sample time h obtained with the use of simulation, described by Table 1 and shown in Fig. 7 is the same as the functions shown in Fig. 8 and 5. It also has a minimum, but the sample time minimizing the settling time is much longer.

Notice also that it is possible to modify the cost function (25) so that it directly expresses the settling time T_c. The proposed modification of $J(h)$ is described underneath. It changes the value of function without changing the localization of the minimum. Let us consider the cost function $\tilde{J}(h) = J(h) + \zeta,\ \zeta \in \mathbb{R}$. From (25) we obtain:

$$\tilde{J}(h) = \frac{e^{-R_a h}}{y_0 c_0} + \frac{R_a e^{-R_a h}}{b_0 (1 - e^{-R_a h})} + \alpha h + \zeta \tag{28}$$

Fig. 9 shows the diagrams of $\tilde{J}(h)$ for $\zeta = 11.1$ and the interpolation polynomial $W_3(h)$, which was obtained with the use of experimental data.

From the diagrams presented in Fig. 9 we can conclude that the modified cost function (28) for $h \in (650, 1000)$, obtained theoretically can be used as a good approximation of the settling time T_c as a function of sample time h in the considered laboratory control system.

8 Conclusions and Open Problems

The final conclusions of the paper can be formulated as follows:

1. During tests of the control system with the discrete dynamic compensator a new, interesting phenomenon was observed. The dependence between the sample time and the settling time was observed both in the real control system and during simulations. Additionally, the diagram of the cost function proposed in (25) is very similar to diagrams describing the dependence of the settling time on the sample time for real case and simulations.
2. An important open problem is to explain the significant difference between the value of sample time minimizing the settling time in simulation and experiments. This difference can be caused by the fact, that the equation (5) and its finite-dimensional approximation used to simulate the control plant in MAT-

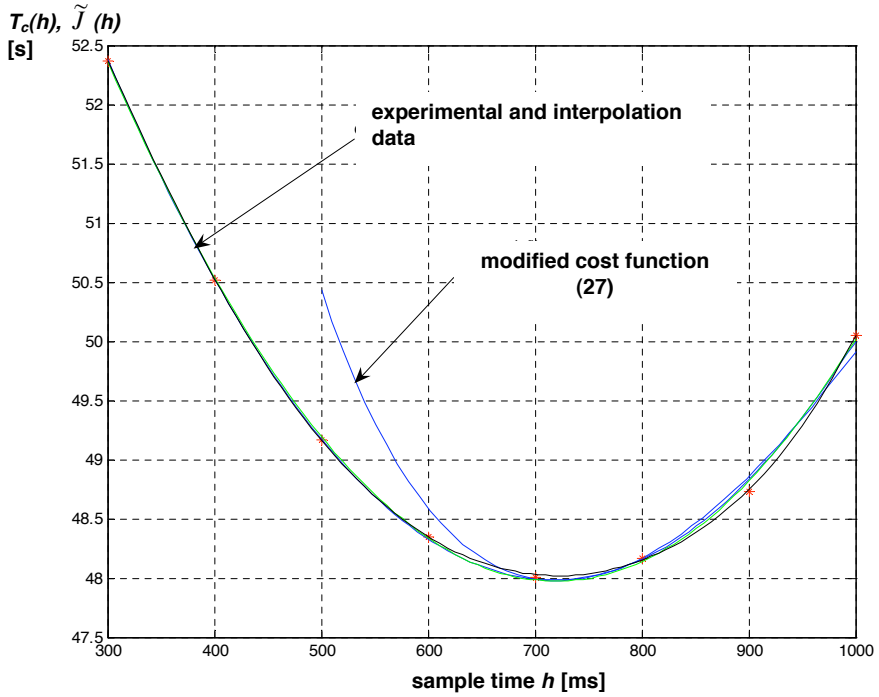

Fig. 9 Comparison of modified cost function $\tilde{J}(h)$ with experimental data and interpolation polynomial $W_3(h)$

LAB are dimensionless in contrast to the real plant. Additionally, the input-output model of the considered system operates only with the use of the standard current signal, although the model describes the heat transfer process, whose measure is temperature. The dependence of the temperature of rod on input and output current signals is very complicated and a knowledge about it is not necessary for the synthesis of the control system for the plant. A correct scaling of the model used to simulations may be the solution of this problem.

3. In the construction of the finite-dimensional compensator the bounded perturbation theorem is applied (see [2], p. 497; [11], p. 79, 81). Relations (12) allow us to use this theorem to the discrete time case.
4. The modified cost function (28) can be applied as a measure of the settling time T_c in real control system. It sufficiently well describes the dependence of the settling time T_c on the model's parameters and the sample time $h > 0$.
5. The relation (28) was proposed after the analysis of the simple model of the considered control plant. It can be helpful to explain the phenomenon of the existence of optimal sample time h_{opt} observed during experiments with the use of real soft PLC control system, presented in Fig. 3. The determining of the parameters α and ξ in modified cost function (28) will be considered by authors in the future.

6. The simulation tests of the function we deal with also confirmed the existence of the sample time minimizing the settling time in the system, but the localization of minimum is significantly different from theoretical and experimental case.
7. As another model of the considered control plant the transfer function with delay can be also considered. It has the following, known form: $G(s) = Ke^{-\tau s}/(Ts+1)$. Its parameters: delay time τ and time constant $T$are relatively simple to identify. During an analysis of this model it was observed that $\alpha \approx 1.2\,\tau$ and $\zeta \approx 0.5\tau$.

Acknowledgements This work was supported by the Ministry of Science and Higher Education of Poland under the Research Project NN 514414034.

References

1. P. Grabowski. An example of identification of a parabolic system. Models with pointwise observation/control. *Prace z Automatyki*, pp. 181–186, Wydawnictwa AGH, Kraków (1997) (in Polish)
2. T. Kato: *Perturbation Theory for Linear Operators*: Springer, Berlin (1980)
3. W. Mitkowski: Stabilization of linear autonomous systems. *Automatyka* **35** (1984) (in Polish)
4. W. Mitkowski. Stabilization of the linear parabolic system with the use of discrete dynamic compensator. *Elektrotechnika* **4**(2) (1985) pp. 189–197 (in Polish)
5. W. Mitkowski: Feedback stabilization of second order evolution equations with damping by discrete-time input-output data. In: *IMACS-IFAC Symp. on Modelling and Simulation for Control of Lumped and Distributed Parameter Systems*, pp 355–358, Lille, France (1986)
6. W. Mitkowski. Stabilization of infinite-dimensional linear systems with the use of dynamic feedback. *Arch. Automatyki i Telemechaniki* 33(4) (1988) pp. 515–528 (in Polish)
7. W. Mitkowski: *Stabilization of Dynamical Systems*: WNT (1991) (in Polish)
8. W. Mitkowski, K. Oprzędkiewicz: Finite dimensional dynamic feedback with bounded control. *Automatyka* **3**(1) (1999) pp. 235–242 (in Polish)
9. K. Oprzędkiewicz: Modeling of parabolic problems in MATLAB/SIMULINK. In *Proc. of III Conf. Comp. Simulation*, Mexico City (1995), pp. 45–49
10. K. Oprzędkiewicz: An example of parabolic system identification. *Elektrotechnika* **16**(2) (1997) pp. 99–106 (in Polish)
11. A. Pazy: *Semigroups of Linear Operators and Applications to Partial Differential Equations*: Springer, New York (1983)
12. Y. Sakawa: Feedback stabilization of linear diffusion systems. *SIAM J. Control and Optimization* **31**(5) (1983) pp. 667–676
13. R. Triggiani: On the stabilization problem in Banach space. *J. Math. Anal. Appl.* **52**(3) (1975) pp. 383–403